Constraints on the application of long chain diol proxies in the Iberian Atlantic margin

Marijke W. de Bar[a], Denise J. C. Dorhout[a], Ellen C. Hopmans[a], Sebastiaan W. Rampen[a], Jaap S. Sinninghe Damsté[a,b] and Stefan Schouten[a,b]

[a] *NIOZ Royal Netherlands Institute for Sea Research, Department of Marine Microbiology and Biogeochemistry, and Utrecht University, P.O. Box 59, 1790 AB Den Burg, Texel, the Netherlands*

[b] *Utrecht University, Faculty of Geosciences, P.O. Box 80115, 3508 TC Utrecht, the Netherlands*

Corresponding author: Marijke de Bar (Marijke.de.Bar@nioz.nl)

Abstract

Long chain diols are lipids that have gained interest over the last years due to their high potential to serve as biomarkers and diol indices have been proposed to reconstruct upwelling conditions and sea surface temperature (SST). However, little is known about the sources of the diols and the mechanisms impacting their distribution. Here we studied the factors controlling diol distributions in the Iberian Atlantic margin, which is characterized by a dynamic continental shelf under the influence of upwelling of nutrient-rich cold deep waters, and fluvial input. We analyzed suspended particulate matter (SPM) of the Tagus river, marine SPM and marine surface sediments along five transects off the Iberian margin, as well as riverbank sediments and soil from the catchment area of the Tagus river. Relatively high fractional abundances of the C_{32} 1,15-diol (normalized with respect to the 1,13- and 1,15-diols) were observed in surface sediments in front of major river mouths and this abundance correlates strongly with the BIT index, a tracer for continental input of organic carbon. Together with an even higher fractional abundance of the C_{32} 1,15-diol in the Tagus river SPM, and the absence of long chain diols in the watershed riverbank sediments and soils, we suggest that this long chain diol is produced *in-situ* in the river. Further support for this hypothesis comes from the small but distinct stable carbon isotopic difference of 1.3‰ with the marine C_{28} 1,13-diol. The 1,14-diols are relatively abundant in surface sediments directly along the northern part of the coast, close to the upwelling zone, suggesting that Diol

Indices based on 1,14-diols would work well as upwelling tracers in this region. Strikingly, we observed a significant difference in stable carbon isotopic composition between the mono-unsaturated $C_{30:1}$ 1,14- and the saturated C_{28} 1,14-diol (3.8±0.7‰), suggesting different sources, in accordance with their different distributions. In addition, the Long chain Diol Index (LDI), a proxy for sea surface temperature, was applied for the surface sediments. The results correlate well with satellite SSTs offshore but reveal a significant discrepancy with satellite-derived SSTs in front of the Tagus and Sado rivers. This suggests that river outflow might compromise the applicability of this proxy.

Keywords

Long chain diols, Long chain Diol Index, Diol Index, 1,13-, 1,14- and 1,15-diols, stable carbon isotopes, Iberian Atlantic margin, upwelling, sea surface temperature, river outflow.

1. Introduction

One of the most important climate parameters that earth scientists try to reconstruct is sea surface temperature (SST). During the last decades, several organic proxies have been developed that have become important tools for climate reconstruction. Two organic proxies are commonly used for the reconstruction of past SSTs: the $U^{K'}_{37}$ index (Brassell et al., 1986; Prahl and Wakeham, 1987) based on the degree of unsaturation of long chain alkenones produced by haptophyte algae, and the TEX_{86} index (Schouten et al., 2002; Kim et al., 2010), based on the distribution of isoprenoid glycerol dialkyl glycerol tetraethers (GDGTs), mainly produced by Thaumarchaeota. Many studies have used alkenones, as these compounds are often abundant in marine sediments, occur worldwide, and are relatively easy to analyze. Since their producers, haptophyte algae, are light dependent and live near the sea surface, the $U^{K'}_{37}$ index shows a good correlation with SST (Muller et al., 1998; Herbert, 2003). However, there are compromising factors such as interspecies variation (Conte et al., 1998), seasonality, habitat depth and oxic degradation (e.g. Hoefs et al., 1998). In contrast to haptophyte algae, Thaumarchaeota are not phototrophic but nitrifiers that depend on ammonium (Könneke et al., 2005; Wuchter et al., 2006), often sourced by the decay of phytoplanktonic organic matter. This means that the TEX_{86} proxy often reflects subsurface water column temperatures rather than SST (Dos Santos et al., 2010; Kim et al., 2012;

Schouten et al., 2013; Chen et al., 2014). In addition, it suffers from similar pitfalls as the $U^{K'}_{37}$ proxy, i.e., uncertainties in seasonality and degradation (e.g. Schouten et al., 2004; 2013; Kim et al., 2009b; Basse et al., 2014). Moreover, riverine continental organic matter input can bias the TEX_{86} signal, although this can be assessed by means of the Branched versus Isoprenoid Tetraether index (BIT), a tracer for fluvial input of soil-derived and riverine organic carbon (e.g. Hopmans et al., 2004; Zell et al., 2013; 2014; De Jonge et al., 2014).

Long chain diols form a group of lipids increasingly investigated over the last decades because of their potential to serve as biomarkers. They were first identified in Black Sea sediments (De Leeuw et al., 1981). This discovery was followed by many studies that reported long chain diols in marine (e.g. Versteegh et al., 1997 and 2000; Hinrichs et al., 1999; Sinninghe Damsté et al., 2003; Rampen et al., 2007; 2008 and 2009) and lacustrine environments (e.g. Xu et al., 2007; Romero-Viana et al., 2012; Rampen et al., 2014b). From culture studies, it has become clear that marine and freshwater eustigmatophyte algae produce 1,13- and 1,15-diols, with chain lengths generally varying between C_{28} and C_{32}. However, their role as source organism of these diols in the marine environment is still uncertain, since the distribution found in marine sediments differs from that found in cultures (Volkman et al., 1992; Versteegh et al., 1997; Rampen et al., 2014b). Apart from 1,13- and 1,15-diols, 1,14 long chain diols are also commonly found in marine sediments. These diols are usually assigned to *Proboscia* diatoms as Sinninghe Damsté et al. (2003) and Rampen et al. (2007) showed that this diatom genus produces saturated and mono-unsaturated C_{28} and C_{30} 1,14-diols. The saturated C_{28}, C_{30} and C_{32} 1,14-diols have also been reported in the marine Dictyochophyte *Apedinella radians* (Rampen et al., 2011). However, the importance of this organism as source for 1,14-diols in the ocean is still unknown.

Recently, a new proxy for past sea surface temperature has been proposed based on the distribution of long chain diols in marine sediments: the Long chain Diol Index (LDI; Rampen et al., 2012). Additionally, the Diol Index (Rampen et al., 2008; Willmott et al., 2010), a proxy for upwelling/high nutrient conditions, has been proposed. The LDI index is based on the fractional abundances of the C_{28} 1,13, C_{30} 1,13- and C_{30} 1,15-diols. Analysis of their distribution in a large set of marine surface sediments derived from all over the world shows that the abundance of these diols correlates strongly with annual mean SST: the C_{30} 1,15-diol has the strongest positive correlation (R^2 =

0.95), whereas the C_{28} and C_{30} 1,13-diols reveal slightly lesser negative correlations (R^2 = 0.88 and R^2 = 0.80, respectively). The C_{32} 1,15-diol does not correlate with SST (R^2 = 0.01). Based on this, the index is defined as the relative abundance of the C_{30} 1,15-diol versus the C_{28} and C_{30} 1,13-diols:

$$\text{Long chain Diol Index (LDI)} = \frac{F_{C_{30}1,15-\text{diol}}}{F_{C_{28}1,13-\text{diol}} + F_{C_{30}1,13-\text{diol}} + F_{C_{30}1,15-\text{diol}}} \quad [1]$$

SST is calculated from the LDI index based on the following relation (Rampen et al., 2012):

$$\text{LDI} = 0.033 \times \text{SST} + 0.095 \quad (R^2 = 0.969;\ n = 162;\ \text{SE} \pm 2\ ^{o}\text{C}) \quad [2]$$

Proboscia diatoms are often associated with high productivity and upwelling conditions (Hernández-Becerril, 1995; Lange et al., 1998; Koning et al., 2001). Their role as the most important 1,14-diol producers under upwelling conditions was confirmed by a sediment trap study in the Arabian Sea (Rampen et al., 2007), and based on this an index for upwelling intensity during the South Western Indian Monsoon was proposed (Rampen et al., 2008):

$$\text{Diol Index 1} = \frac{[C_{28} + C_{30}\ 1,14\ \text{diols}]}{([C_{28} + C_{30}\ 1,14\ \text{diols}] + [C_{30}\ 1,15\ \text{diol}])} \quad [3]$$

A second upwelling index was proposed by (Willmott et al., 2010), for the Western Bransfield Basin (Antarctica) since the C_{28} and C_{30} 1,13-diols were more abundant than the C_{30} 1,15-diol:

$$\text{Diol Index 2} = \frac{[C_{28} + C_{30}\ 1,14\ \text{diols}]}{([C_{28} + C_{30}\ 1,14\ \text{diols}] + [C_{28} + C_{30}\ 1,13\ \text{diols}])} \quad [4]$$

Preliminary application in sediment cores of the LDI and the two Diol Indices have shown their promise as proxies (Naafs et al., 2012; Rampen et al., 2012; 2014a; Seki et al., 2012; Lopes dos Santos et al., 2013; Smith et al., 2013; Rodrigo-Gamiz et al., 2014; Nieto-Moreno et al., 2015; Plancq et al., 2015). However, there are still uncertainties in the application of these biomarkers and it is crucial that additional studies are done to improve the reliability of these proxies. For example, studies have related increased abundances of *Proboscia* to stratified conditions rather than upwelling (e.g. Fernández and Bode, 1994). Indeed, Contreras et al. (2010) observed increased concentrations of the C_{28} 1,14-diol in the Peruvian upwelling system during times of stratification (interglacials) and low concentrations during times of upwelling.

Here we tested the long chain diol proxies in surface sediments from the Atlantic Iberian margin. Previous organic geochemical work in this region has shown the presence of long chain diols in surface sediments (Schmidt et al., 2010). This region experiences upwelling during summer and downwelling during winter due to the northerly and southerly trade winds and the Azores high pressure system driving the surface circulation. Additionally, the margin receives freshwater input from different rivers, of which the two largest are the Tagus and Douro. We analyzed long chain diols in surface sediments of 5 transects along the Iberian margin (Fig. 1D). Transect I and IV are located in front of the Douro and Tagus, respectively, allowing the ability to assess the potential influence of fluvial input on the long chain diol proxies. Transects II and V start in the estuaries of the smaller Mondego and Sado rivers, respectively, and transect III is not under the influence of riverine input. The results shed light on the applicability of long chain diol proxies in a coastal environment under the influence of a seasonal upwelling system, and with terrestrial input via riverine transport.

2. Materials and methods

2.1 Site description

The Atlantic Iberian margin is characterized by a steep slope dissected by different submarine canyons, of which the most important are the Nazaré, Cascais and Setúbal-Lisbon canyons (e.g. Vanney and Mougenot, 1981). The shelf is relatively narrow, ranging between 20 and 50 km in width. The shelf break is located at a water depth of around 140 m (Mougenot, 1988). The surface ocean circulation off the Western Iberian Peninsula is driven by the Portugal Current (PC) System. The PC is a slow equatorward current (e.g. Martins et al., 2002). Between May and September (summer upwelling), the Portugal Coastal Current (PCC), along the coast dominates. This current is flowing southward induced by northerly Portugal trade winds and the Azores anticyclone moving towards the Iberian Peninsula (e.g. Fiúza et al., 1982; Martins et al., 2002). As a result, the cold, nutrient-rich subsurface water rises to the surface along the Iberian margin, leading to increased productivity (Fiúza, 1983). Fig. 1B shows the influence of upwelling waters during summer, lowering the SST, particularly in the northern part of the region (off the Douro river). Between September and October, the surface circulation is reversed by the dominance of the poleward Portugal Coastal Countercurrent (PCCC) driven by the southerly winds,

which persist until April (winter downwelling season) (Álvarez-Salgado et al., 2003 and references therein). In January and February, another phytoplankton bloom occurs due to the large discharge of nutrients from the rivers (Dias et al., 2002), although less intense as compared to the plankton blooms associated with summer upwelling.

The two largest rivers delivering nutrients to shelf are the Douro and Tagus (Fig. 1D). The Tagus river has a length of ca. 1000 km, being the longest river of the Iberian Peninsula, with a watershed of about 80.600 km^2 (Jouanneau et al., 1998). The river forms an important source of freshwater input to the continental shelf and includes a large estuary with an area of around 300 to 340 km^2 (Vale and Sundby, 1985). Whereas the mean annual water discharge is around 360 $m^3 s^{-1}$, this discharge ranges between 80 and 720 $m^3 s^{-1}$ due to inter-annual variation, and between 1 and 2200 $m^3 s^{-1}$ on a seasonal scale, due to pronounced dry and wet seasons (Loureiro and Macedo, 1986; Jouanneau et al., 1998). There is a region of persistent high productivity in front of the Tagus river mouth, as evidenced by high chlorophyll concentrations (Fig. 1C; Moita et al., 2003). The Douro, located in the NW of the Iberian Peninsula, with a drainage basin of 95.700 km^2 has an annual mean water discharge of 500 $m^3 s^{-1}$ (Van der Leeden, 1975), and also shows a strong seasonality. Upwelling in front of the Douro shows a large offshore extent, as can be deduced from chlorophyll images (Alt-Epping et al., 2007; Fig. 1C). These dynamic conditions lead to the deposition of sandy sediments (Dias and Nitrouer, 1984). However, there are also deposits of fine-grained sediments, located offshore of the Douro and Tagus river inlets, mainly fed by the two rivers. Off the Douro, this so-called mud belt is around 500 km^2 large and 2 to 5 m thick, and it is located on the mid-shelf around a depth of 90 m (McCave, 1972; Araújo et al., 1994; Drago et al., 1998; 1999; Vitorino et al., 2002). The mud belt off the Tagus estuary covers the continental shelf from the estuary to the shelfbreak. This mud patch results from estuarine deposition, with an area of 560 km^2 and maximum thickness of 25 m (Rodrigues and Matos (1994) cited by Jouanneau et al., 1998). This deposit is confined by the incisions of the Lisbon and Setubal Canyons, delivering river sediment to the basin (Jouanneau et al., 1998). Other rivers entering the Iberian surface ocean, relevant for this study, are the Sado (mean annual discharge < 10 $m^3 s^{-1}$; Loureiro et al., 1986) and the Mondego (mean annual discharge of 82 $m^3 s^{-1}$; Van der Leeden, 1975; Fig. 1D).

169

170 *2.2 Sample collection and lipid analysis*

171 Marine suspended particulate matter (SPM) and sediment samples were collected during the
172 PACEMAKER 64PE332 cruise with the R/V Pelagia, between 14th and 29th March 2011 (see Zell et al.,
173 2014, 2015). Sediment cores from 31 stations were retrieved from five transects (Fig. 1D) going from
174 inshore to offshore. The top 0.5 cm of the multi-cores were used in this study. Additional to the surface
175 sediments, SPM was collected at three stations of transect I and at four stations of transect IV at different
176 water depths. SPM from the Tagus river mouth was sampled over one year, every month (July 2011
177 until June 2012, with exception of August 2011; water depth 0 m; sample location indicated by the star
178 symbol in Fig. 1D). Additionally, 16 surface soils and 10 riverbank sediments from the Tagus river
179 watershed were sampled from the source to the mouth of the river in 2012 (for sample locations and
180 description, see Zell et al., 2014). The complete sample set has been previously studied for glycerol
181 dialkyl glycerol tetraethers (GDGTs) (Zell et al., 2014, 2015).

182 Extracts prepared and described by Zell et al. (2014, 2015) were reanalyzed for this study. Soil,
183 riverbank sediments and marine surface sediments (~2 g dry weight) were extracted using Accelerated
184 Solvent Extraction (ASE), and subsequently separated over an activated Al_2O_3 column into an apolar
185 and polar fraction, using hexane:dichloromethane (DCM) (1:1, v:v) and DCM:methanol (MeOH) (1:1,
186 v:v), respectively. Marine and river SPM samples were also previously extracted using a modified Bligh
187 and Dyer (BD) technique following (Pitcher et al., 2009). These extracts were separated in core lipid
188 (CL) and intact polar lipid (IPL) fractions over an activated silica gel column, using hexane:ethyl acetate
189 (1:1, v:v) and MeOH as eluents, respectively (Oba et al., 2006; Pitcher et al., 2009). Subsequently, the
190 CL fractions were separated over Al_2O_3 into an apolar and polar fractions, using hexane:DCM (1:1, v:v)
191 and DCM:MeOH (1:1, v:v), respectively. For diol analysis, these existing polar fractions were silylated
192 by means of addition of BSTFA (*N*,*O*-bis(trimethylsilyl)trifluoroacetamide) and pyridine, and heating
193 at 60 ^{0}C for 20 min. Subsequently, the samples were dissolved in ethyl acetate and injected on-column
194 on an Agilent 7890B gas chromatograph (GC) coupled to an Agilent 5977A mass spectrometer (MS).
195 The samples were injected at 70 ^{0}C. The oven temperature was programmed to 130 ^{0}C by 20 ^{0}C min^{-1},
196 and subsequently to 320 ^{0}C by 4 ^{0}C min^{-1}; this temperature was held for 25 min. The GC was equipped

with an on-column injector and fused silica column (25 m x 0.32 mm) coated with CP Sil-5 (film thickness 0.12 µm). Helium was used as carrier gas at a constant flow of 2 mL min^{-1}. The mass spectrometer operated with an ionization energy of 70 eV and a cycle time of 1.9 s. The injection volume was 1 µL. The long chain diols were quantified in selective ion monitoring (SIM) mode scanning of their characteristic fragments, i.e., *m/z* 299, 313, 327 and 341, with a gain factor of 3 and a dwell time of 100 ms per target ion. Identity confirmation was done in full scan mode by means of the characteristic fragmentation spectra (Versteegh et al., 1997). All samples were analyzed in duplicate, and some in triplicate with a mean SD of 0.01 for Diol Index 1 (Rampen et al., 2008), a mean SD of 0.02 for Diol Index 2 (Willmott et al., 2010), and a mean SD of 0.02 for the LDI, corresponding to 0.6 ^{0}C based on the calibration of Rampen et al. (2012). Distribution plots were created in Ocean Data View (ODV; Schlitzer, 2015) using the DIVA gridding algorithm.

2.3 Compound-specific stable carbon isotope analysis

Stable carbon isotopes were measured on isolated long chain diols from the surface sediment of the first station of transect V, indicated by the red circle in Fig. 1D. For this purpose, the upper 1 cm core-top sediment (23.4 g dry weight) of this station was used. The sediment was homogenized and extracted by ASE with a DCM:MeOH (9:1, v/v) mixture to obtain the total lipid extract (TLE). Solvent was removed under a stream of nitrogen. The TLE was subsequently redissolved in DCM and water was removed over anhydrous Na_2SO_4, after which the extracts were dried under a stream of nitrogen. The extract was separated by column chromatography. Activated (at 150 °C for 2 h) Al_2O_3 was used as stationary phase, using DCM and DCM/MeOH (1:1, v/v) as eluents to yield the apolar and polar fraction, respectively.

Since diols of the same chain length but different mid-chain positions of the alcohol groups coelute upon gas chromatographic separation, it was not possible to analyze the isotopic composition of individual isomers by GC-IRMS directly. Becker et al. (2015) previously demonstrated separation of diols with different mid-chain positions of the alcohol group using normal phase HPLC. We therefore applied semi-preparative normal phase HPLC to separate diols with differing mid-chain positions of the alcohol group prior to isotope analysis. The polar fraction was prepared for semi-preparative normal

phase HPLC by dissolving in hexane/isopropanol (99:1. v/v) and filtration over a polytetrafluoroethylene (PTFE) filter (0.45 µm pore size, Grace, USA). The polar fraction (8.9 mg) was then fractionated by high performance liquid chromatography (HPLC) using an Agilent 1100 series HPLC (Agilent Technologies, USA) equipped with a fraction collector (ISCO Foxy Jr, Teledyne ISCO, USA). Separation of the diol isomers was achieved over a semi-preparative silica column (250 mm x 10 mm; 10 µm; Alltech Econosphere, Grace, USA) at room temperature. Diols were eluted with 86% A and 14% B for the first 35 min, followed by a gradient to 100% B in 1 min, kept for 30 min, after which B was brought back to 14%. A = hexane and B = hexane/isopropanol (9:1, v/v). The flow was kept constant at 3 mL min^{-1}. Thirty second fractions were collected, of which a small aliquot (~2%) was analyzed for diols using GC-MS in SIM mode as described above. Diols eluted between 10 and 40 minutes. The fractions that were pooled together to isolate a certain diol isomer are highlighted by the rectangles surrounding the fractions (Fig. 3) and these pooled fractions were used to measure the individual $\delta^{13}C$ of the diol isomers. In this manner, the mono-unsaturated $C_{30:1}$ 1,14-diol, the saturated C_{32} 1,15-, C_{28} 1,13- and C_{28} 1,14-diol were isolated and analyzed by GC-IRMS. Purity of the isolated product was assessed by means of GC-MS in full scan mode (*m/z* 50-800).

Isotopic composition of the isolated diols was analyzed using gas chromatography – isotope ratio mass spectrometry (GC-IRMS). For this the diols were silylated, as described above, using BSTFA with a known $\delta^{13}C$ value of -32.2±0.5‰. The samples were analyzed on a Thermo Delta V isotope ratio monitoring mass spectrometer coupled to an Agilent 6890 GC. The GC conditions are the same as described for the GC-MS above. The samples were analyzed in triplicate; the reported data represent averaged values, and are reported in delta notation relative to the VPDB standard using CO_2 reference gas calibrated to the NBS-22 reference material. The instrument error was <0.3‰ based on repeated injection of external deuterated *n*-alkane standards (C_{20} and C_{24} perdeuterated *n*-alkanes) prior to and after sample analysis. Correction for the addition of the labelled trimethylsilyl groups was achieved via the following equation:

$$\delta^{13}C_{DC}\ (‰\ \text{VPDB}) = \frac{(C_{DC}\times\delta^{13}C_{COM})-(C_{BSTFA}\times\delta^{13}C_{BSTFA})}{C_{COM}} \quad [5]$$

where $\delta^{13}C_{DC}$ is the $\delta^{13}C$ of the derivatised compound, C_{DC} the carbon number of the derivatised

compound, $\delta^{13}C_{COM}$ the $\delta^{13}C$ of the underivatised compound, C_{BSTFA} the number of carbon atoms added by the BSTFA, $\delta^{13}C_{BSTFA}$ the $\delta^{13}C$ value of the BSTFA (-32.2‰), and C_{COM} the carbon number of the underivatised compound (Rieley, 1994). This correction leads to an additional uncertainty of ca. ±0.2‰.

3 Results

3.1 Long chain diol distributions

3.1.1 Marine sediments and SPM

All 31 surface sediments contained detectable amounts of long chain diols, although the abundances were generally low. Long chain diols were not detected in the marine SPM. For the 1,13- and 1,15-diols, the dominant chain lengths were C_{28}, C_{30} and C_{32}, and for the 1,14-diols these were C_{28} and C_{30} (Table 1). The mono-unsaturated $C_{30:1}$ 1,14-diol and saturated C_{28} 1,14-diol were detected in only a few sediments. The $C_{30:1}$ 1,14-diol was mainly detected close to the coastline, whereas the C_{28} 1,14-diol was also observed offshore. Besides diols, the C_{30} and C_{32} keto-ols (Versteegh et al., 1997) and the C_{29} 12-hydroxy methyl alkanoate (Sinninghe Damsté et al., 2003) were detected in all sediments. The fractional abundance of the C_{32} 1,15-diol (normalized with respect to all diols) ranged between 0.05 and 0.23 with the highest values at the Tagus river mouth, and overall higher fractional abundances along the coast and lower abundances further offshore (Fig. 3). The C_{30} 1,14-diol had the highest fractional abundance (up to 0.91) directly along the coast (especially the northern part), while the C_{30} 1,15-diol and C_{28} 1,13-diol showed the opposite trend with higher abundances (up to 0.52 and 0.28, respectively) in open ocean surface sediments and lower abundances (0.10 and 0.05, respectively) along the Portuguese margin (Fig. 2). Accordingly, both upwelling indices based on diols (Eq. 3 and 4) were highest along the coastline (especially in the northern part) and decreased offshore (Figs. 5A-B). Diol Index 1 (Rampen et al., 2008) ranged between 0.87 and 0.26, and Diol Index 2 (Willmott et al., 2010) ranged between 0.83 and 0.40. LDI values varied between 0.33 and 0.69, corresponding with SSTs varying between 7 and 18 ^{0}C. The distribution plot of the LDI values (Fig. 5E) shows the lowest LDI values in front of the Tagus and Sado river, and higher LDI values offshore compared to onshore.

280

281 3.1.2. Riverine SPM and sediments

282 For the riverine SPM, the same long chain diols were detected as in the marine surface sediments
283 except for the C_{28} 1,13- and 1,14-diol and the $C_{30:1}$ 1,14-diol, which were not detected. Also, the C_{29} 12-
284 hydroxy methyl alkanoate was not detected. However, we did identify the C_{32} 1,17-diol which was not
285 detected in the marine surface sediments. Between 67 and 89% of the long chain diols was made up by
286 the C_{30} and C_{32} 1,15-diol, while the C_{32} 1,17-diol contributed between 11 and 27%. The C_{30} 1,13- and
287 1,14-diols had much lower fractional abundances compared to the marine surface sediments (Table 1).
288 The relatively high fractional abundance of the C_{32} 1,15-diol, ranging between 0.25 and 0.50 is notable.
289 LDI values could not be calculated due to the absence of the C_{28} 1,13-diol. Values for the diol upwelling
290 indices were generally lower than in marine sediments, ranging between 0.03 - 0.10 for Diol Index 1
291 (Rampen et al., 2008) and between 0.20 - 0.49 for Diol Index 2 (Willmott et al., 2010). Long chain diols
292 were not detected in the riverbank sediments or in the soils of the river watershed.

293

294 *3.2 Compound specific carbon isotopes*

295 To determine the origin of long chain diols in the Portuguese margin, we analyzed the stable
296 carbon isotopic composition of several diol isomers in the core top sediment of the first station of transect
297 V in front of the Sado (indicated by a red dot in Fig. 1D). Prior to stable isotope analysis the diol isomers
298 were isolated by preparative HPLC since on GC-IRMS diols of the same chain length but different
299 position of the alcohol position co-elute. Mass spectrometry analysis did not reveal co-eluting diol
300 isomers in the pooled fractions of the C_{32} 1,15- and $C_{30:1}$ 1,14-diol. The pooled C_{28} 1,13-diol fraction
301 contained a minor amount (3%) of the co-eluting C_{28} 1,14-diol, and the C_{28} 1,14-diol fraction contained
302 some (12%) co-eluting C_{28} 1,13-diol. Isotopic analysis showed that the C_{32} 1,15-diol had the most ^{13}C-
303 enriched value ($\delta^{13}C$ = -31.3±0.7‰), followed by the C_{28} 1,13-diol ($\delta^{13}C$ = -32.6±0.5‰), while the C_{28}
304 1,14- and $C_{30:1}$ 1,14-diols were more depleted in ^{13}C ($\delta^{13}C$ = -34.6±0.4‰ and -38.4±0.4‰, respectively).

305 It is known that separation by HPLC can potentially cause isotopic fractionation and lead to
306 erroneous $\delta^{13}C$ values if the compounds are not quantitatively recovered (Caimi and Brenna, 1997). To
307 constrain this issue we isolated a pure C_{28} 1,13-diol standard using the identical approach as described

above and its isotopic composition was compared to that determined directly by GC-IRMS. The 7 collection vials over which this standard became distributed contained 99.8% of the starting material. The stable carbon isotopic variation across the chromatographic peak showed, as expected, relatively ^{13}C-depleted molecules eluting at the front of the peak and relatively ^{13}C-enriched molecules eluting in the tail (Fig. 4). Based on this experiment we estimate that when >80% of a long chain diol is isolated, isotopic fraction due to semi-preparative HPLC is < 0.5‰, i.e., within the analytical error of a typical GC-IRMS analysis. In our study, we isolated > 80% for all diol isomers analyzed by GC-IRMS.

4. Discussion

4.1 Sources of 1,14-diols and the applicability of the Diol Indices

The 1,14-diols have been reported in *Proboscia* diatoms (Sinninghe Damsté et al., 2003; Rampen et al., 2007) and in the alga *Apedinella radians* of the Dictyochophyceae phylum (Rampen et al., 2011). *Proboscia* has been confirmed as a likely source of long chain 1,14-diols (Rampen et al., 2008), but the importance of *Apedinella* as source of 1,14-diols in the ocean is still uncertain. Here, all the marine sediments contained the C_{29} 12-OH-methyl alkanoate, which is a typical biomarker for *Proboscia* diatoms (Sinninghe Damsté et al., 2003). Furthermore, we detected the mono-unsaturated $C_{30:1}$ 1,14-diol, present in *Proboscia* diatoms, but not the C_{32} 1,14-diol, which is present in *Apedinella radians* (Rampen et al., 2011). Additionally, two studies have reported *Proboscia alata* diatoms along the west coast of Portugal (Schott et al., 1997; Moita et al., 2003). Finally, the low fractional abundance of 1,14 diols in the Tagus river SPM (between 1 and 4% of total long chain diol assemblage; Table 1) is consistent with a predominant marine source for these diols, i.e., *Proboscia* diatoms.

To reinforce that the 1,14-diols derive from a different source than the 1,13- and 1,15-diols, the stable carbon isotope values for C_{28} 1,13-, C_{28} 1,14-, $C_{30:1}$ 1,14- and the C_{32} 1,15-diol were determined. The 1,14-diols were depleted in ^{13}C by 2.0 to 7.1‰ compared to the 1,13- and 1,15-diols in the sediments. Sinninghe Damsté et al. (2003) determined the δ^{13}C values of the C_{28} 1,14-diol (predominantly 1,14-isomer), $C_{30:1}$ 1,14-diol, C_{32}-diol (60% 1,15-isomer, 40% 1,17 isomer) and the C_{30} diol in an Arabian Sea sediment. Similar to our results, they observed that the 1,14-diols were depleted

in ^{13}C relative to the 1,13- and 1,15-diols in the sediments (by 1.5 to 5.2‰), and that the C_{32}-diol was most enriched in ^{13}C relative to the other diols measured. The fact that the 1,14 diols are isotopically distinct from the 1,13- and 1,15-diols supports the hypothesis that they are derived from different sources. Interestingly, the $\delta^{13}C$ values of the C_{28} and $C_{30:1}$ 1,14-diols differed by ca. 4‰, suggesting that these compounds may be produced by different organisms. Alternatively, these compounds are produced by the same organism, but have biosynthetically induced different carbon isotope compositions. However, Sinninghe Damsté et al. (2003) found only a small (~1‰) isotopic offset between 1,14 diol isomers measured for a *P. indica* culture. This suggests that the large isotopic discrepancy which we observe between the C_{28} and $C_{30:1}$ 1,14-diols, is likely due to different source organisms (e.g. a different *Proboscia* source). This is in agreement with the different distributions of these diols in the surface sediments, as the $C_{30:1}$ 1,14-diol was only detected close to the coastline (coinciding with high abundances of the saturated C_{30} 1,14-diol), whereas the C_{28} 1,14-diol was more abundant offshore.

Both Diol Index 1 (Rampen et al., 2008) and Diol Index 2 (Willmott et al., 2010) are relatively high along the northern part of the coastal studied area, and decrease further away from the coast (Figs. 5A-5B). This fits well with the coastal upwelling during summer (Figs. 1B-C), potentially with *Proboscia alata* blooms, suggesting the Diol Indices reflect summer upwelling in this region. Thus, both Diol Indices seem to be applicable here. It has been previously shown by Rampen et al. (2014a) that Diol Index 1 is also affected by temperature and therefore not suitable as a global upwelling index. However, since the SST gradient is relatively small (ca. 2 ^{0}C) in our study area, this has likely not affected the applicability of the index here in this region.

4.2 Sources of the C_{32} 1,15-diol

From our core top dataset, it is clear that the highest fractional abundance of the C_{32} 1,15-diol is near the river mouth of the Tagus (Table 1; Fig. 2E). However, when we consider the fractional abundance of this diol only with respect to the C_{28} 1,13- , C_{30} 1,13- and C_{30} 1,15-diol (i.e., normalize on the diol assemblage without the 1,14-diols so that we compare compounds potentially all derived from the same source), it becomes evident that its fractional abundance is also high in front of the river mouth

of the Douro (Fig. 5D). This distribution of the fractional abundance of the C_{32} 1,15-diol is remarkably similar to that reported for the BIT index (Zell et al., 2015) (Figs. 5C-D) and the two proxies correlate well ($R^2 = 0.62$; $p < 0.001$). Since the BIT index is a proxy for the input of soil and riverine organic matter transported from land into the marine realm (Hopmans et al., 2004; Huguet et al., 2006; Walsh et al., 2008; Kim et al., 2009a; Zell et al., 2013; 2014; De Jonge et al., 2014), this could suggest that the C_{32} 1,15-diol is predominantly derived from land. Zell et al. (2015) showed for the Tagus river that the declining brGDGT concentrations with increasing distance from the river is the main factor in the declining BIT. Indeed, there is a strong correlation between the fractional abundance of the C_{32} 1,15-diol and the sum of non-cyclized brGDGTs (brGDGTs used in the BIT index; $R^2 = 0.78$, $n = 30$; $p < 0.001$; Fig. 6). A riverine source of the C_{32} 1,15-diol is confirmed by the high relative abundances of this long chain diol in the Tagus river SPM: the average fractional abundance of the C_{32} 1,15-diol (with respect to the 1,13- and 1,15-diols) is 0.46, coinciding with an average BIT index of 0.71 (Zell et al., 2015). Collectively these data suggest that the C_{32} 1,15 diol is transported by rivers to the marine environment. Interestingly, we have not detected any long chain diols in the soils in the watershed of the river, or in the riverbank sediments, suggesting that the C_{32} 1,15-diol is not produced in soils but *in situ* in the river itself. Fig. 7 shows the fractional abundances of the different diol isomers detected in the Tagus river SPM. Seemingly, the C_{32} 1,15-diol reveals an opposite pattern compared to the other diols, with highest fractional abundance during winter. This might suggest that the C_{32} 1,15-diol derives from a different source. Also the C_{32} 1,17-diol, solely detected in the river SPM, reveals an opposite trend as compared to the C_{32} 1,15-diol, with lowest fractional abundance during winter. Consequently, this also implies that the C_{32} 1,15-diol and C_{32} 1,17-diol are likely to be produced by different source organisms.

Results of previous studies support our hypothesis of a possible additional freshwater source for the C_{32} 1,15-diol in coastal marine environments. Versteegh et al. (1997) developed a diol index, defined as the ratio of the C_{30} 1,15-diol over the sum of the C_{30} 1,15- and C_{32} 1,15-diol and observed that the index was generally lower, implying relative high abundances of the C_{32} 1,15-diol, in freshwater sediments compared to the ocean sediments. Indeed, the C_{32} 1,15-diol is often the most abundant diol in lake sediments (Xu et al., 2007; Castañeda et al., 2009; Shimokawara et al., 2010; Romero-Viana et al.,

2013; Rampen et al., 2014a). Furthermore, Versteegh et al. (2000) observed higher relative abundances of the C_{32} 1,15-diol and -keto-ol below the Congo River plume, while Rampen et al. (2014b) observed high fractional abundances of the C_{32} 1,15-diol in sediments of the Hudson Bay, which is a large inland sea in Canada, strongly influenced by riverine input. Collectively, this suggests that the C_{32} 1,15-diol might be a good tracer for the relative amount of fluvial input into coastal marine environments. However, to confirm this hypothesis, further studies of other coastal regions are needed.

Additional reinforcement of the hypothesis that the C_{32} 1,15-diol might derive from rivers comes from the stable carbon isotopic composition. The C_{32} 1,15-diol is, with a $\delta^{13}C$ value of -31.3‰, the most enriched in ^{13}C compared to other diols, and differs by 1.3‰ relative to the C_{28} 1,13-diol, generally assumed to be produced by the same organism. However, this difference is relatively small (on the edge of significance: two-tailed $p = 0.053$; measurement and instrument error 0.8 and 0.3‰) and it is not known yet how $\delta^{13}C$ values of different diol isomers vary within algal species. Therefore, culture studies are needed to assess if this truly signifies a different source or whether it reflects biosynthetic differences.

4.3 Long chain Diol Index (LDI)

We compared our LDI-derived SST data with satellite annual mean SSTs (from Kim et al., 2010). In this region, annual mean SST varies between ca. 15 and 17 ^{0}C, with a latitudinal temperature gradient, i.e., a decreasing SST from North to South. However, the LDI-derived SSTs revealed a much larger range of ca. 7 to 17 ^{0}C. Indeed, there is a poor correlation between the LDI-derived SST and satellite SST ($R^2 = 0.18$, $n = 31$; $p < 0.019$). Fig. 5F shows the spatial distribution of the mismatch between the calculated LDI temperatures and the mean annual SST. For most sediments, in particular offshore sediments, the offset was less than the 2 ^{0}C, the standard error of the estimate of the LDI (Rampen et al., 2012), suggesting that the LDI reflects mean annual SST. LDI temperature estimates offshore (~16-17 °C) agree best with annual mean SST (~16-17 °C), as winter SST offshore varies between ~14 and 15.5 °C and summer SST between ~18 and 20 °C. We observed mismatches of -3 to -4 ^{0}C between LDI SSTs and satellite annual mean SSTs along the coast line in front of the Douro and

Mondego, and consequently LDI-derived SSTs agree better with winter SST. The LDI-derived temperatures in the Tagus prodelta and Sado estuary showed the largest offset of up to -9 ^{0}C compared to the annual mean SST, and up to -7 ^{0}C relative to winter SST. This large temperature difference is unlikely to result from cold deeper water rising to the surface during summer upwelling, since upwelling mainly occurs northward off the Douro, and upwelling conditions might lower SST by only ca. 2 ^{0}C (Fig. 1B). Moreover, the gradient in LDI SST estimates around the Tagus seems to trace the river outflow out of the Tagus and Sado estuary. Since the Tagus has the highest discharge during winter it might be that the outflow of cold river water simply lowers the seawater temperature. However, this would also be evident from satellite SST, and we would expect the same effect for the Douro. Alternatively, it might be that the offset between LDI-derived temperatures and satellite SSTs is the result of an input of diols derived from the river. Based on our analysis of riverine SPM, it is likely that, apart from the C_{32} 1,15-diol, the river delivers other diols to the shelf region. Averaged over the sampling year, the C_{30} 1,15-diol was slightly higher in abundance than the C_{32} 1,15-diol in the river SPM, so we would also expect to observe a riverine contribution of this diol into the marine realm. However, the relative abundance of the C_{30} 1,15-diol in the surface sediments is lowest in front of the rivers, and increases offshore. Moreover, a contribution of this diol would lead to a much higher LDI rather than lower. Furthermore, the C_{32} 1,17-diol (detected in Tagus river SPM) was not detected in the surface sediments in front of the Tagus river mouth. Therefore, it is unlikely that the input of riverine diols is an explanation for the offset in the values of the LDI in the areas affected by riverine input.

There is no substantial gradient in the annual mean salinity resulting from river outflow (Kim et al., 2016), and seasonal variations in salinity in the Tagus prodelta are relatively small (Bartels-Jónsdóttir et al., 2008), hence, it is unlikely that the proxy signal is affected by changes in salinity in this region. Possibly, the marine diol producers present in the region of the Tagus and Sado river outflows are different from those near the Douro and in the open ocean due to the input of (micro)nutrients. Indeed, chlorophyll-*a* data reveal that there is persistently high productivity offshore of the mouth of the Tagus (e.g. Fig. 1C), as induced by summer, as well as the less intense winter upwelling, and the year-round discharge of the Tagus river (e.g. Alt-Epping et al., 2008). Off the Douro, coastal upwelling is likely the most important source for nutrients. Further research examining other coastal marine

environments with large fluvial inputs is needed to investigate whether the LDI is compromised in these regions.

5. Conclusions

In this study, we have explored the long chain diol distributions along the Iberian Atlantic margin. The two Diol Indices, based on the relative abundance of the 1,14-diols, were applied to test their applicability as upwelling indicators and both indices seemed to work well in this region. Carbon isotope analysis of different diol isomers implies that the 1,14-diols have different sources than the 1,13- and 1,15-diols. However, we observed a large isotopic discrepancy between the $C_{30:1}$ 1,14-diol and the C_{28} 1,14-diol (3.8±0.8‰), suggesting different sources.

Whereas offshore the LDI-based SST values are close to satellite mean annual SST, near-shore we observe large discrepancies in front of the Douro and Mondego rivers (-3 to -4 ^{0}C), but especially in the Tagus prodelta and Sado estuary with temperature offsets of up to -9 ^{0}C. This offset is likely not caused by the input of diols derived from the rivers, as the diol distribution in SPM of the Tagus river suggests that river contribution would lead to higher temperatures rather than lower. Possibly, freshwater and nutrient input from the Tagus and Sado rivers creates conditions in which different organisms proliferate as compared to the rest of the shelf and the open ocean, leading to these different diol distributions in the sediments. Further research is essential to assess whether fluvial input compromises the LDI proxy in other regions.

High fractional abundances of the C_{32} 1,15-diol in front of the Douro and Tagus rivers and in the Tagus river SPM as well as a strong correlation with the BIT suggest that it is partly derived from the continent. The absence of long chain diols in riverbank sediments and watershed soils, leads to the hypothesis that the C_{32} 1,15-diol is predominantly produced *in situ* in rivers. Stable carbon isotope analysis of this diol supports this hypothesis, since we obtain an isotopic difference of 1.3 ‰ relative to the marine C_{28} 1,13-diol. However, culture studies are needed to assess whether this small isotopic offset is indeed the result of different sources.

Acknowledgements

We thank Anchelique Mets and Monique Verweij for analytical support, and Claudia Zell, Jung-Hyun Kim, Jérôme Bonnin and Marianne Baas for sampling. We thank an anonymous reviewer, Dr. Rodrigo-Gamiz and Dr, Elizabeth Canuel for useful comments which have improved the manuscript. The crew of the R/V Pelagia is thanked for their services. This research has been funded by the European Research Council (ERC) under the European Union's Seventh Framework Program (FP7/2007-2013) ERC grant agreement [339206] to S.S. S.S. and J.S.S.D. receive financial support from the Netherlands Earth System Science Centre (NESSC).

References

Alt-Epping, U., 2008. Late Quaternary sediment processes and sediment accumulation changes off Portugal, Dissertation Universität Bremen, 161 pp.

Alt-Epping, U., Mil-Homens, M., Hebbeln, D., Abrantes, F., Schneider, R.R., 2007. Provenance of organic matter and nutrient conditions on a river- and upwelling influenced shelf: A case study from the Portuguese margin. Marine Geology 243, 169-179.

Alvarez-Salgado, X.A., Figueiras, F.G., Perez, F.F., Groom, S., Nogueira, E., Borges, A., Chou, L., Castro, C.G., Moncoiffe, G., Rios, A.F., Miller, A.E.J., Frankignoulle, M., Savidge, G., Wollast, R., 2003. The Portugal coastal counter current off NW Spain: new insights on its biogeochemical variability. Progress in Oceanography. 56, 281-321.

Araújo, M.F., Dias, J.M.A., Jouanneau, J.M., 1994. Chemical characterisation of the main fine sedimentary deposit at the northwestern Portuguese shelf. Gaia 9, 59-65.

Bartels-Jónsdóttir, H.B., Voelker, A.H.L., Knudsen, K.L., Abrantes, F., 2009. Twentieth-century warming and hydrographical changes in the Tagus Prodelta, eastern North Atlantic. Holocene 19, 369-380.

Basse, A. , Zhu, C. , Versteegh, G. J. , Fischer, G. , Hinrichs, K. U., Mollenhauer, G., 2014. Distribution of intact and core tetraether lipids in water column profiles of suspended particulate matter off Cape Blanc, NW Africa , Organic Geochemistry 72, 1-13.

Becker, K.W., Lipp, J.S., Versteegh, G.J.M., Wormer, L., Hinrichs, K.U., 2015. Rapid and simultaneous analysis of three molecular sea surface temperature proxies and application to sediments from the Sea of Marmara. Organic Geochemistry 85, 42-53.

Brassell, S.C., Eglinton, G., Marlowe, I.T., Pflaumann, U., Sarnthein, M., 1986. Molecular stratigraphy - a new tool for climatic assessment. Nature 320, 129-133.

Caimi, R.J., Brenna, J.T., 1997. Quantitative evaluation of carbon isotopic fractionation during reversed-phase high-performance liquid chromatography. Journal of Chromatography A 757, 307-310.

Castaneda, I.S., Werne, J.P., Johnson, T.C., 2009. Influence of climate change on algal community structure and primary productivity of Lake Malawi (East Africa) from the Last Glacial Maximum to present. Limnology and Oceanography 54, 2431-2447.

Chen, W.W., Mohtadi, M., Schefuss, E., Mollenhauer, G., 2014. Organic-geochemical proxies of sea surface temperature in surface sediments of the tropical eastern Indian Ocean. Deep Sea Research Part I: Oceanographic Research Papers 88, 17-29.

Conte, M.H., Thompson, A., Lesley, D., Harris, R.P., 1998. Genetic and physiological influences on the alkenone/alkenoate versus growth temperature relationship in Emiliania huxleyi and Gephyrocapsa oceanica. Geochimica et Cosmochimica Acta 62, 51-68.

Contreras, S., Lange, C.B., Pantoja, S., Lavik, G., Rincon-Martinez, D., Kuypers, M.M.M., 2010. A rainy northern Atacama Desert during the last interglacial. Geophysical Research Letters 37, L23612.

De Jonge, C., Stadnitskaia, A., Hopmans, E.C., Cherkashov, G., Fedotov, A., Sinninghe Damsté, J.S., 2014. In situ produced branched glycerol dialkyl glycerol tetraethers in suspended particulate matter from the Yenisei River, Eastern Siberia. Geochimica et Cosmochimica Acta 125, 476-491.

De Leeuw, J.W., Rijpstra, W.I.C., Schenck, P.A., 1981. The occurence and identification of C_{30}, C_{31} and C_{32} alkan-1,15-diols and alkan-15-one-1-ols in Unit I and Unit-II Black Sea sediments. Geochimica et Cosmochimica Acta 45, 2281-2285.

Dias, J.M.A., Jouanneau, J.M., Gonzalez, R., Araujo, M.F., Drago, T., Garcia, C., Oliveira, A., Rodrigues, A., Vitorino, J., Weber, O., 2002. Present day sedimentary processes on the northern Iberian shelf. Progress in Oceanography 52, 249-259.

Dias, J.M.A., Nittrouer, C.A., 1984. Continental shelf sediments of northern Portugal. Continental Shelf Research 3, 147–165.

Dos Santos, R.A.L., Prange, M., Castaneda, I.S., Schefuss, E., Mulitza, S., Schulz, M., Niedermeyer, E.M., Sinninghe Damsté, J.S., Schouten, S., 2010. Glacial-interglacial variability in Atlantic meridional overturning circulation and thermocline adjustments in the tropical North Atlantic. Earth and Planetary Science Letters 300, 407-414.

Drago, T., Araújo, F., Valério, P., Weber, O., Jouanneau, J. M., 1999. Geomorphological control of fine sedimentation on the northern Portuguese shelf. Boletin Instituto Espagnol Oceanografia 15, 111–122.

Drago, T., Oliveira, A., Magalhães, F., Cascalho, J., Jouanneau, J.M., Vitorino, J., 1998. Some evidence of the northward fine sediment transport in the northern Portuguese continental shelf. Oceanologica Acta 21, 223–231.

542 European Commission, Joint Research Centre (2016): EMIS - SeaWiFS Monthly sea surface
543 Chlorophyll-a concentration (2km) in mg m^{-3}. European Commission, Joint Research
544 Centre (JRC). Dataset accessed on 25/08/2016.
545 Fernández, E., Bode, A., 1994. Succession of phytoplankton assemblages in relation to the hydrography
546 in the southern Bay of Biscay: a multivariate approach. Scientia Marina 58, 191-205.
547 Fiúza, A., 1983. Upwelling patterns off Portugal. In: Suess, E., Thide, J. (Eds.) Coastal upwelling, its
548 sediment record: Responses of sedimentary regime to present coastal upwelling. Nato
549 Conference Series 10B, Springer, 58–89.
550 Fiuza, A.F.D., Demacedo, M.E., Guerreiro, M.R., 1982. Climatological space and time-variation of the
551 Portuguese coastal upwelling. Oceanologica acta 5, 31-4
552 Herbert, T.D., 2003. Alkenone Paleotemperature Determinations. In: Turekian, K.K., Holland, H.D.
553 (Ed.), Treatise on Geochemistry. Elsevier-Pergamon, Oxford, pp. 391-432.
554 Hernández-Becerril, D.U., 1995. Planktonic diatoms from the Gulf of California and coasts off Baja
555 California: The genera Rhizosolenia, Proboscia, Pseudosolenia, and former Rhizosolenia
556 species. Diatom Research 10, 251-267.
557 Hinrichs, K.U., Schneider, R.R., Muller, P.J., Rullkotter, J., 1999. A biomarker perspective on
558 paleoproductivity variations in two Late Quaternary sediment sections from the Southeast
559 Atlantic Ocean. Organic Geochemistry 30, 341-366.
560 Hoefs, M.J.L., Versteegh, G.J.M., Rijpstra, W.I.C., De Leeuw, J.W., Sinninghe Damsté, J.S., 1998.
561 Postdepositional oxic degradation of alkenones: Implications for the measurement of palaeo sea
562 surface temperatures. Paleoceanography 13, 42-49.
563 Hopmans, E.C., Weijers, J.W.H., Schefuss, E., Herfort, L., Sinninghe Damsté, J.S., Schouten, S., 2004.
564 A novel proxy for terrestrial organic matter in sediments based on branched and isoprenoid
565 tetraether lipids. Earth and Planetary Science Letters 224, 107-116.
566 Huguet, C., Hopmans, E.C., Febo-Ayala, W., Thompson, D.H., Sinninghe Damsté, J.S., Schouten, S.,
567 2006. An improved method to determine the absolute abundance of glycerol dibiphytanyl
568 glycerol tetraether lipids. Organic Geochemistry 37, 1036-1041.
569 Jouanneau, J.M., Garcia, C., Oliveira, A., Rodrigues, A., Dias, J.A., Weber, O., 1998. Dispersal and
570 deposition of suspended sediment on the shelf off the Tagus and Sado estuaries, SW Portugal.
571 Progress in Oceanography 42, 233-257.
572 Kim, J.H., Buscail, R., Bourrin, F., Palanques, A., Sinninghe Damsté, J.S., Bonnin, J., Schouten, S.,
573 2009a. Transport and depositional process of soil organic matter during wet and dry storms on
574 the Tet inner shelf (NW Mediterranean). Paleogeography, Paleoclimatology, Paleoecology 273,
575 228-238.

Kim, J.H., Crosta, X., Willmott, V., Renssen, H., Bonnin, J., Helmke, P., Schouten, S., Sinninghe Damsté, J.S., 2012. Holocene subsurface temperature variability in the eastern Antarctic continental margin. Geophysical Research Letters 39.

Kim, J.H., Huguet, C., Zonneveld, K.A.F., Versteegh, G.J.M., Roeder, W., Sinninghe Damsté, J.S., Schouten, S., 2009b. An experimental field study to test the stability of lipids used for TEX_{86} and $U^{K'}_{37}$ palaeothermometry. Geochimica et Cosmochimica Acta 73, 2888-2898.

Kim, J.H., van der Meer, J., Schouten, S., Helmke, P., Willmott, V., Sangiorgi, F., Koc, N., Hopmans, E.C., Sinninghe Damsté, J.S., 2010. New indices and calibrations derived from the distribution of crenarchaeal isoprenoid tetraether lipids: Implications for past sea surface temperature reconstructions. Geochimica et Cosmochimica Acta 74, 4639-4654.

Kim, J.H., Villanueva, L., Zell, C., Sinninghe Damsté, J.S., 2016. Biological source and provenance of deep-water derived isoprenoid tetraether lipids along the Portuguese continental margin. Geochimica et Cosmochimica Acta 172, 177-204.

Koning, E., van Iperen, J.M., van Raaphorst, W., Helder, W., Brummer, G.J.A., van Weering, T.C.E., 2001. Selective preservation of upwelling-indicating diatoms in sediments off Somalia, NW Indian Ocean. Deep Sea Research Part I: Oceanographic Research Papers 48, 2473-2495.

Konneke, M., Bernhard, A.E., de la Torre, J.R., Walker, C.B., Waterbury, J.B., Stahl, D.A., 2005. Isolation of an autotrophic ammonia-oxidizing marine archaeon. Nature 437, 543-546.

Lange, C.B., Romero, O.E., Wefer, G., Gabric, A.J., 1998. Offshore influence of coastal upwelling off Mauritania, NW Africa, as recorded by diatoms in sediment traps at 2195 m water depth. Deep Sea Research Part I: Oceanographic Research Papers 45, 985-1013.

Lopes dos Santos, R.A., Spooner, M.I., Barrows, T.T., De Deckker, P., Sinninghe Damsté, J.S., Schouten, S., 2013. Comparison of organic ($U^{K'}_{37}$, TEX^{H}_{86}, LDI) and faunal proxies (foraminiferal assemblages) for reconstruction of late Quaternary sea-surface temperature variability from offshore southeastern Australia. Paleoceanography 28, 377-387.

Loureiro, J.J.M., Macedo, M.E., 1986. Bacia Hidrografica do Rio Tejo. Monografias Hidrologicas dos Principais Cursos de Agua de Portugal continental, Servico Hidraulico (DGRAH), Lisbon, 281-335.

Loureiro, J.J., Machado, M.L., Macedo, M.E., Nunes, M.N., Botelho, O.F., Sousa, M.L., Almeida, M.C., Martins, J.C., 1986. Direcção Geral dos Serviços Hidraulicos. Monografias hidrológicas dos principais cursos de água de Portugal Continental., Lisboa, p. 569.

Martins, C.S., Hamann, M., Fiuza, A.F.G., 2002. Surface circulation in the eastern North Atlantic, from drifters and altimetry. Journal of Geophysical Research 107, 3217.

McCave, I.N., 1972. Transport and escape of fine-grained sediment from shelf areas. In: Swift, D. J. P., Duane, D. B., Pilkey, O. H. (Eds). Shelf sediment transport: processes and patterns. Stroudsburg, PA: Dowden, Hutchinson & Ross, pp 225-248.

Moita, M.T., Oliveira, P.B., Mendes, J.C., Palma, A.S., 2003. Distribution of chlorophyll a and Gymnodinium catenatum associated with coastal upwelling plumes off central Portugal. Acta Oecologica 24, S125-S132.

Mougenot, D., 1988. Géologie de la marge portugaise. These Doct. d'Etat. Univ. Paris VI.

Muller, P.J., Kirst, G., Ruhland, G., von Storch, I., Rosell-Mele, A., 1998. Calibration of the alkenone paleotemperature index $U^{K'}_{37}$ based on core-tops from the eastern South Atlantic and the global ocean (60 degrees N-60 degrees S). Geochimica et Cosmochimica Acta 62, 1757-1772.

Naafs, B.D.A., Hefter, J., Stein, R., 2012. Application of the long chain diol index (LDI) paleothermometer to the early Pleistocene (MIS 96). Organic Geochemistry 49, 83-85.

Nieto-Moreno, V., Martínez-Ruiz, F., Gallego-Torres, D., Giralt, S., García-Orellana, J., Masqué, P., Sinninghe Damsté, J.S., Ortega-Huertas, M., 2015. Palaeoclimate and palaeoceanographic conditions in the westernmost Mediterranean over the last millennium: an integrated organic and inorganic approach. Journal of the Geological Society 172, 264-271.

Oba, M., Sakata, S., Tsunogai, U., 2006. Polar and neutral isopranyl glycerol ether lipids as biomarkers of archaea in near-surface sediments from the Nankai Trough. Organic Geochemistry 37, 1643-1654.

Pitcher, A., Hopmans, E.C., Schouten, S., Sinninghe Damsté, J.S., 2009. Separation of core and intact polar archaeal tetraether lipids using silica columns: Insights into living and fossil biomass contributions. Organic Geochemistry 40, 12-19.

Plancq, J., Grossi, V., Pittet, B., Huguet, C., Rosell-Mele, A., Mattioli, E., 2015. Multi-proxy constraints on sapropel formation during the late Pliocene of central Mediterranean (southwest Sicily). Earth and Planetary Science Letters 420, 30-44.

Prahl, F.G., Wakeham, S.G., 1987. Calibration of unsaturation patterns in long chain ketone compositions for paleotemperature assessment. Nature 330, 367-369.

Rampen, S.W., Datema, M., Rodrigo-Gamiz, M., Schouten, S., Reichart, G.J., Sinninghe Damsté, J.S., 2014b. Sources and proxy potential of long chain alkyl diols in lacustrine environments. Geochimica Et Cosmochimica Acta 144, 59-71.

Rampen, S.W., Schouten, S., Koning, E., Brummer, G.J.A., Sinninghe Damsté, J.S., 2008. A 90 kyr upwelling record from the northwestern Indian Ocean using a novel long chain diol index. Earth and Planetary Science Letters 276, 207-213.

Rampen, S.W., Schouten, S., Schefuss, E., Sinninghe Damsté, J.S., 2009. Impact of temperature on long chain diol and mid-chain hydroxy methyl alkanoate composition in Proboscia diatoms: Results from culture and field studies. Organic Geochemistry 40, 1124-1131.

Rampen, S.W., Schouten, S., Sinninghe Damsté, J.S., 2011. Occurrence of long chain 1,14-diols in Apedinella radians. Organic Geochemistry 42, 572-574.

Rampen, S.W., Schouten, S., Wakeham, S.G., Sinninghe Damsté, J.S., 2007. Seasonal and spatial variation in the sources and fluxes of long chain diols and mid-chain hydroxy methyl alkanoates in the Arabian Sea. Organic Geochemistry 38, 165-179.

Rampen, S.W., Willmott, V., Kim, J.H., Rodrigo-Gamiz, M., Uliana, E., Mollenhauer, G., Schefuss, E., Sinninghe Damsté, J.S., Schouten, S., 2014a. Evaluation of long chain 1,14-alkyl diols in marine sediments as indicators for upwelling and temperature. Organic Geochemistry 76, 39-47.

Rampen, S.W., Willmott, V., Kim, J.H., Uliana, E., Mollenhauer, G., Schefuss, E., Sinninghe Damsté, J.S., Schouten, S., 2012. Long chain 1,13-and 1,15-diols as a potential proxy for palaeotemperature reconstruction. Geochimica Et Cosmochimica Acta 84, 204-216.

Rieley, G., 1994. Derivatization of organic-compounds prior to gas-chromatographic combustion-isotope ratio mass-spectrometric analysis - identification of isotope fractionation processes. Analyst 199, 915-919.

Rodrigo-Gamiz, M., Martinez-Ruiz, F., Rampen, S.W., Schouten, S., Sinninghe Damsté, J.S., 2014. Sea surface temperature variations in the western Mediterranean Sea over the last 20 kyr: A dual-organic proxy ($U^{K'}_{37}$ and LDI) approach. Paleoceanography 29, 87-98.

Rodrigues, A., Matos, M. (1994). Distribuçao sedimentar do plataforma continentale portuguese entre Sines e Ericeira. 1st Symposio Margem Continental Iberica Atlantica. Abstract, 48.

Romero-Viana, L., Kienel, U., Sachse, D., 2012. Lipid biomarker signatures in a hypersaline lake on Isabel Island (Eastern Pacific) as a proxy for past rainfall anomaly (1942-2006 AD). Paleogeography, Paleoclimatology, Paleoecology 350, 49-61.

Romero-Viana, L., Kienel, U., Wilkes, H., Sachse, D., 2013. Growth-dependent hydrogen isotopic fractionation of algal lipid biomarkers in hypersaline Isabel Lake (México). Geochimica Et Cosmochimica Acta 106, 490-500.

Salgueiro, E., Voelker, A., Abrantes, F., Meggers, H., Pflaumann, U., Loncaric, N., Gonzalez-Alvarez, R., Oliveira, P., Bartels-Jonsdottir, H.B., Moreno, J., Wefer, G., 2008. Planktonic foraminifera from modern sediments reflect upwelling patterns off Iberia: Insights from a regional transfer function. Marine Micropaleontology 66, 135-164.

Schlitzer, R., 2015. Ocean Data View, odv.awi.de.

Schmidt, F., Hinrichs, K.-U., Elvert, M., 2010. Sources, transport, and partitioning of organic matter at a highly dynamic continental margin. Marine Chemistry 118, 37-55.

Schott, F., Koltermann, K.P., Stramma, L., SY, A., Zahn, R., Zenk, W., 1998. North Atlantic, cruise 39, 18 April - 14 September 1997. METEOR-Berichte, Universität Hamburg, 197 pp.

Schouten, S., Hopmans, E.C., Schefuss, E., Sinninghe Damsté, J.S., 2002. Distributional variations in marine crenarchaeotal membrane lipids: a new tool for reconstructing ancient sea water temperatures? Earth and Planetary Science Letters 204, 265-274.

682 Schouten, S., Hopmans, E.C., Sinninghe Damsté, J.S., 2004. The effect of maturity and depositional
683 redox conditions on archaeal tetraether lipid palaeothermometry. Organic Geochemistry 35,
684 567-571.
685 Schouten, S., Hopmans, E.C., Sinninghe Damsté, J.S., 2013. The organic geochemistry of glycerol
686 dialkyl glycerol tetraether lipids: A review. Organic Geochemistry 54, 19-61.
687 Seki, O., Schmidt, D.N., Schouten, S., Hopmans, E.C., Sinninghe Damsté, J.S., Pancost, R.D., 2012.
688 Paleoceanographic changes in the Eastern Equatorial Pacific over the last 10 Myr.
689 Paleoceanography 27.
690 Shimokawara, M., Nishimura, M., Matsuda, T., Akiyama, N., Kawai, T., 2010. Bound forms,
691 compositional features, major sources and diagenesis of long chain, alkyl mid-chain diols in
692 Lake Baikal sediments over the past 28,000 years. Organic Geochemistry 41, 753-766.
693 Sinninghe Damsté, J.S., Rampen, S., Irene, W., Rupstra, C., Abbas, B., Muyzer, G., Schouten, S., 2003.
694 A diatomaceous origin for long chain diols and mid-chain hydroxy methyl alkanoates widely
695 occurring in Quaternary marine sediments: Indicators for high-nutrient conditions. Geochimica
696 Et Cosmochimica Acta 67, 1339-1348.
697 Smith, M., De Deckker, P., Rogers, J., Brocks, J., Hope, J., Schmidt, S., Lopes dos Santos, R., Schouten,
698 S., 2013. Comparison of $U^{K'}_{37}$, $TEX^{H}_{86}$and LDI temperature proxies for reconstruction of south-
699 east Australian ocean temperatures. Organic Geochemistry 64, 94-104.
700 Vale, C., Sundby, B., 1987. Suspended sediment fluctuations in the Tagus estuary on semi-diurnal and
701 fortnightly time scales. Estuarine, Coastal and Shelf Science 25, 495-508.
702 Van der Leeden, F., 1975. Water resources of the world: selected statistics. Water Information Center,
703 Port Washington, N.Y., 808.
704 Vanney, J.R., Mougenot, D., 1981. La plate-forme continentale de Portugal et les provinces adjacentes:
705 Analyse geomorphologique. Memoriás dos Serviçios Geológicos de Portugal 28, 86.
706 Versteegh, G.J.M., Bosch, H.J., De Leeuw, J.W., 1997. Potential palaeoenvironmental information of
707 C_{24} to C_{36} mid-chain diols, keto-ols and mid-chain hydroxy fatty acids; a critical review. Organic
708 Geochemistry 27, 1-13.
709 Versteegh, G.J.M., Jansen, J.H.F., De Leeuw, J.W., Schneider, R.R., 2000. Mid-chain diols and keto-
710 ols in SE Atlantic sediments: A new tool for tracing past sea surface water masses? Geochimica
711 Et Cosmochimica Acta 64, 1879-1892.
712 Vitorino, J., Oliveira, A., Jouanneau, J.M., Drago, T., 2002. Winter dynamics on the northern Portuguese
713 shelf. Part 2: bottom boundary layers and sediment dispersal. Progress in Oceanography 52,
714 155-170.
715 Volkman, J.K., Barrett, S.M., Dunstan, G.A., Jeffrey, S.W., 1992. C_{30}-C_{32} alkyl diols and unsaturated
716 alcohols in microalgae of the class Eustigmatophyceae. Organic Geochemistry 18, 131-138.
717 Walsh, E.M., Ingalls, A.E., Keil, R.G., 2008. Sources and transport of terrestrial organic matter in
718 Vancouver Island fjords and the Vancouver-Washington Margin: A multiproxy approach using

719 delta C-13(org), lignin phenols, and the ether lipid BIT index. Limnology and Oceanography
720 53, 1054-1063.
721 Willmott, V., Rampen, S.W., Domack, E., Canals, M., Sinninghe Damsté, J.S., Schouten, S., 2010.
722 Holocene changes in Proboscia diatom productivity in shelf waters of the north-western
723 Antarctic Peninsula. Antarctic Science 22, 3-10.
724 Wuchter, C., Abbas, B., Coolen, M.J.L., Herfort, L., van Bleijswijk, J., Timmers, P., Strous, M., Teira,
725 E., Herndl, G.J., Middelburg, J.J., Schouten, S., Damste, J.S., 2006. Archaeal nitrification in the
726 ocean. Proceedings of the National Academy of Sciences U. S. A. 103, 12317-12322.
727 Xu, Y.P., Simoneit, B.R.T., Jaffe, R., 2007. Occurrence of long chain n-alkenols, diols, keto-ols and
728 sec-alkanols in a sediment core from a hypereutrophic, freshwater lake. Organic Geochemistry
729 38, 870-883.
730 Zell, C., Kim, J.H., Balsinha, M., Dorhout, D., Fernandes, C., Baas, M., Sinninghe Damsté, J.S., 2014.
731 Transport of branched tetraether lipids from the Tagus River basin to the coastal ocean of the
732 Portuguese margin: consequences for the interpretation of the MBT'/CBT paleothermometer.
733 Biogeosciences 11, 5637-5655.
734 Zell, C., Kim, J.H., Dorhout, D., Baas, M., Sinninghe Damsté, J.S., 2015. Sources and distributions of
735 branched tetraether lipids and crenarchaeol along the Portuguese continental margin:
736 Implications for the BIT index. Continental Shelf Research 96, 34-44.
737 Zell, C., Kim, J.H., Moreira-Turcq, P., Abril, G., Hopmans, E.C., Bonnet, M.P., Sobrinho, R.L.,
738 Sinninghe Damsté, J.S., 2013. Disentangling the origins of branched tetraether lipids and
739 crenarchaeol in the lower Amazon River: Implications for GDGT-based proxies. Limnology
740 and Oceanography 58, 343-353.

Fig. 1. Mean satellite-derived SST (°C) between 1985 and 2003 for the Portuguese margin during A) winter and B) summer, modified from Salgueiro et al. (2008) who integrated Pathfinder satellite measurements with a 9 km resolution (version 4.1; data from http://podaac-www.jpl.nasa.gov/sst/). Note the different axis scales. Major currents are indicated in panel A: the Portugal Current (PC), Portugal Coastal Current (PCC) and the Portugal Coastal Countercurrent (PCCC). The upper right panel (C) shows average chlorophyll-*a* concentrations during April 2001. Visible are the high productivity zones along the Portuguese coast as result of upwelling and river discharge delivering nutrients into the ocean (SeaWiFS satellite data; http://emis.jrc.ec.europa.eu/). The lower panel (D) shows the study area with the sample locations of the surface sediments along the five transects. The star symbol indicates SPM sampling in the Tagus river mouth, and the red filled circle reflects the station used for stable carbon isotope analysis.

Fig. 2. Distribution plots for the five major long chain diols normalized with respect to all diols (Table 1). Maps drawn in Ocean Data View, and modified manually.

Fig. 3. A stacked column chart reflecting the distribution of long chain diols in fractions prepped by HPLC of a surface sediment (transect V, indicated by red dot in the map of Fig. 1D). The long chain diols were separated based on position of the mid-chain alcohol. Compound identification was achieved by analyzing every collection vial (every half minute) on GC-MS (the bars represent the different collection vials). The isolation of the diols after semi-preparative HPLC led to the additional detection of the C_{31} 1,15-diol. The long chain diols selected for pooling and subsequent compound specific carbon analysis are highlighted by the 4 different colored boxes: $C_{30:1}$ 1,14-, $C_{32:0}$ 1,15-, $C_{28:0}$ 1,14- and $C_{28:0}$ 1,13-diol, from left to right.

Fig. 4. The upper panel shows the variation in stable carbon isotopic composition across the chromatographic peak of the C_{28} 1,13-diol synthetic standard. The *x*-axis is the percentage of the total compound eluted, and the *y*-axis represents the offset from the $\delta^{13}C$ value of the prepped C_{28} 1,13-diol fractions versus the starting material. The dashed curve represents a third order polynomial fit. The lower panel shows the chromatographic peak (on LC) separated over 11 semi-preparative collection vials of which the C_{28} 1,13-diol of the central 7 collection vials was analyzed by GC-IRMS.

Fig. 5. Distribution plot of (A) Diol Index 1, (B) Diol index 2, (C) the BIT index, (D) the fractional relative abundance ('*F*') of the C_{32} 1,15-diol relative to the fractional abundances of the C_{28} 1,13- and C_{30} 1,13- and 1,15-diols, (E) the Long chain Diol Index (LDI) and (F) the difference in absolute temperature (^{0}C) between the LDI sea surface temperature estimates and the actual satellite mean annual SSTs. Maps drawn in Ocean Data View, and modified manually.

Fig. 6. Fractional abundance (*'F'*) of the C_{32} 1,15-diol (relative to the fractional abundances of the C_{28} 1,13- and C_{30} 1,13- and 1,15-diols) in marine surface sediments versus the summed concentration of the main brGDGTs (Zell et al., 2015).

Fig. 7. The fractional abundances of the different diol isomers measured in the Tagus River suspended particulate matter over 2011 – 2012.

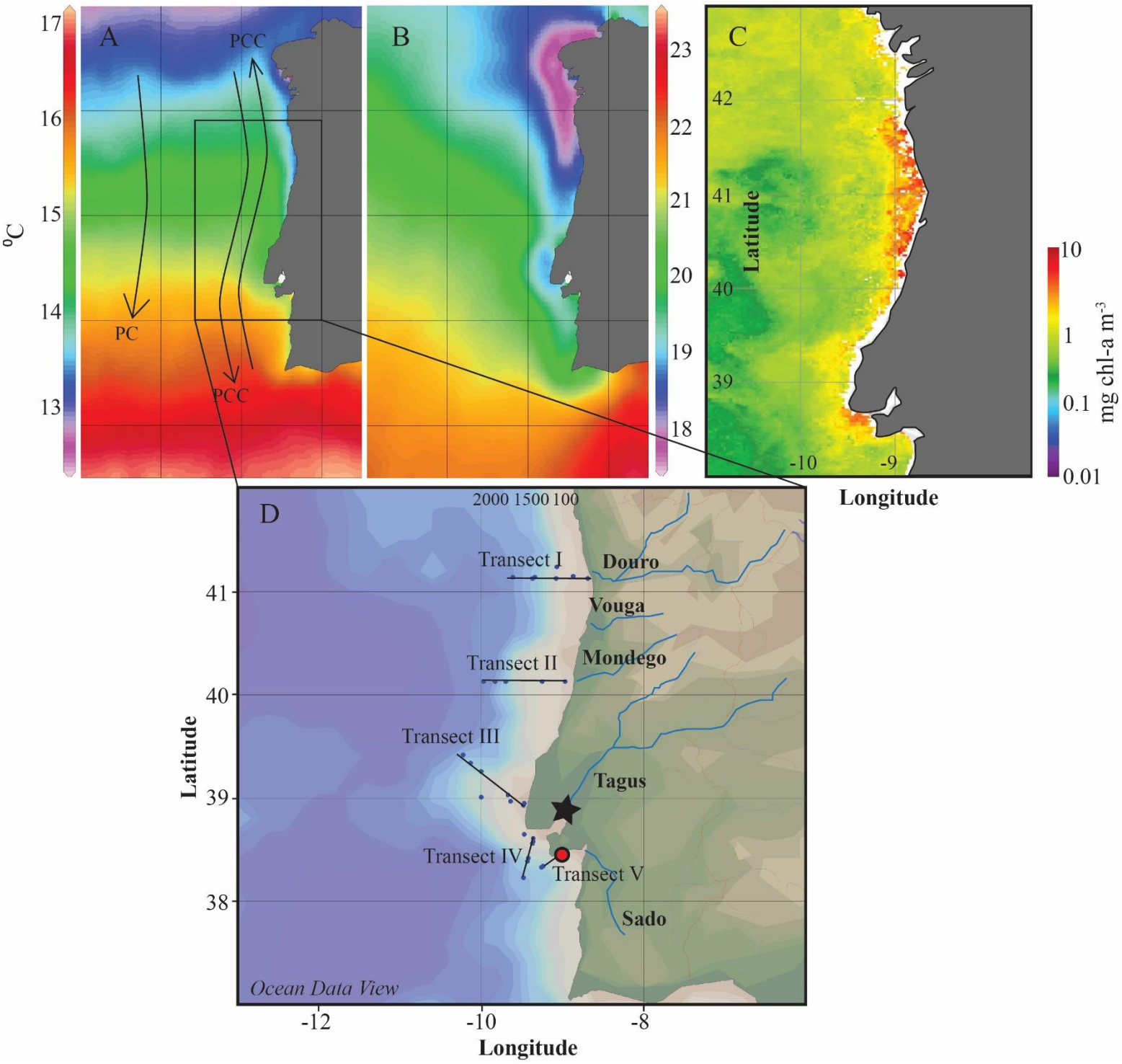
A
PCC
PC
PCC
B
C
42
41
40
39
Latitude
-10
-9
Longitude
°C
17
16
15
14
13
23
22
21
20
19
18
10
1
0.1
0.01
mg chl-a m-3
D
2000 1500 100
Transect I
Douro
Vouga
Transect II
Mondego
Transect III
Tagus
Transect IV
Transect V
Sado
Ocean Data View
41
40
39
38
Latitude
-12
-10
-8
Longitude

785

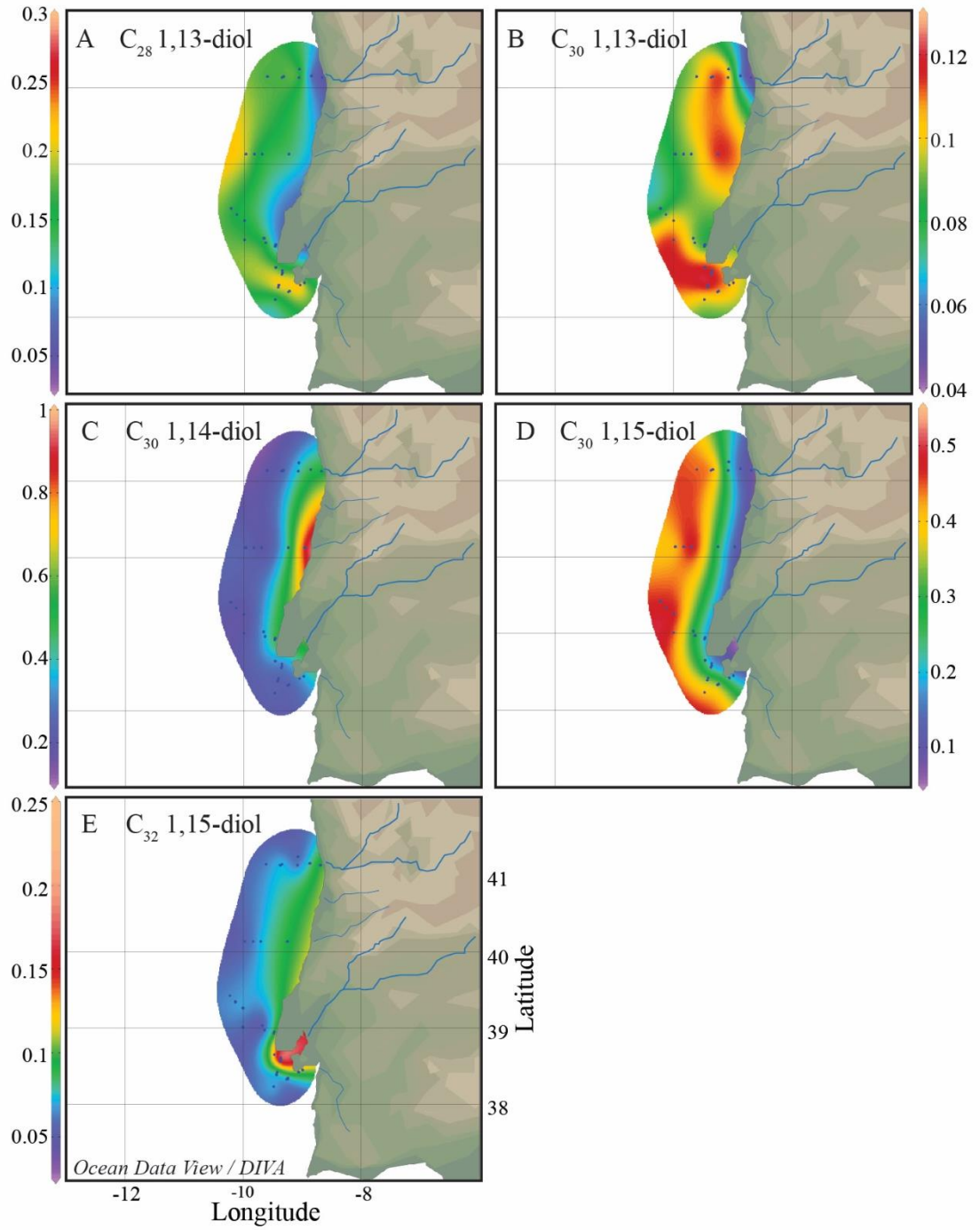
A C28 1,13-diol
B C30 1,13-diol
C C30 1,14-diol
D C30 1,15-diol
E C32 1,15-diol
0.3
0.25
0.2
0.15
0.1
0.05
0.12
0.1
0.08
0.06
0.04
1
0.8
0.6
0.4
0.2
0.5
0.4
0.3
0.2
0.1
0.25
0.2
0.15
0.1
0.05
41
40
39
38
Latitude
Ocean Data View / DIVA
-12
-10
-8
Longitude

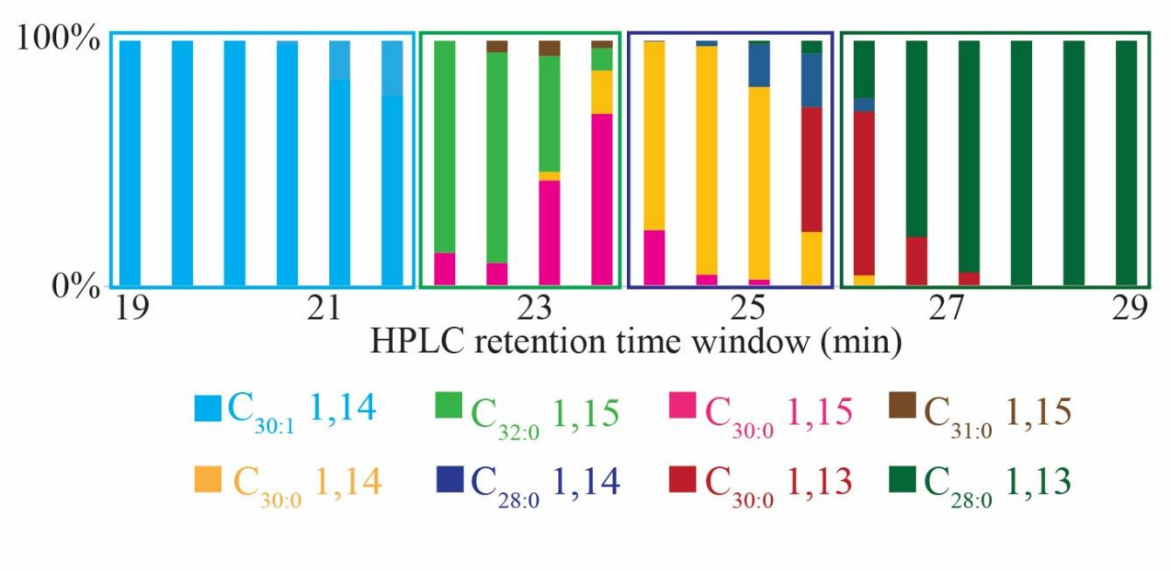
100%
0%
19
21
23
25
27
29
HPLC retention time window (min)
C30:1 1,14
C32:0 1,15
C30:0 1,15
C31:0 1,15
C30:0 1,14
C28:0 1,14
C30:0 1,13
C28:0 1,13

792

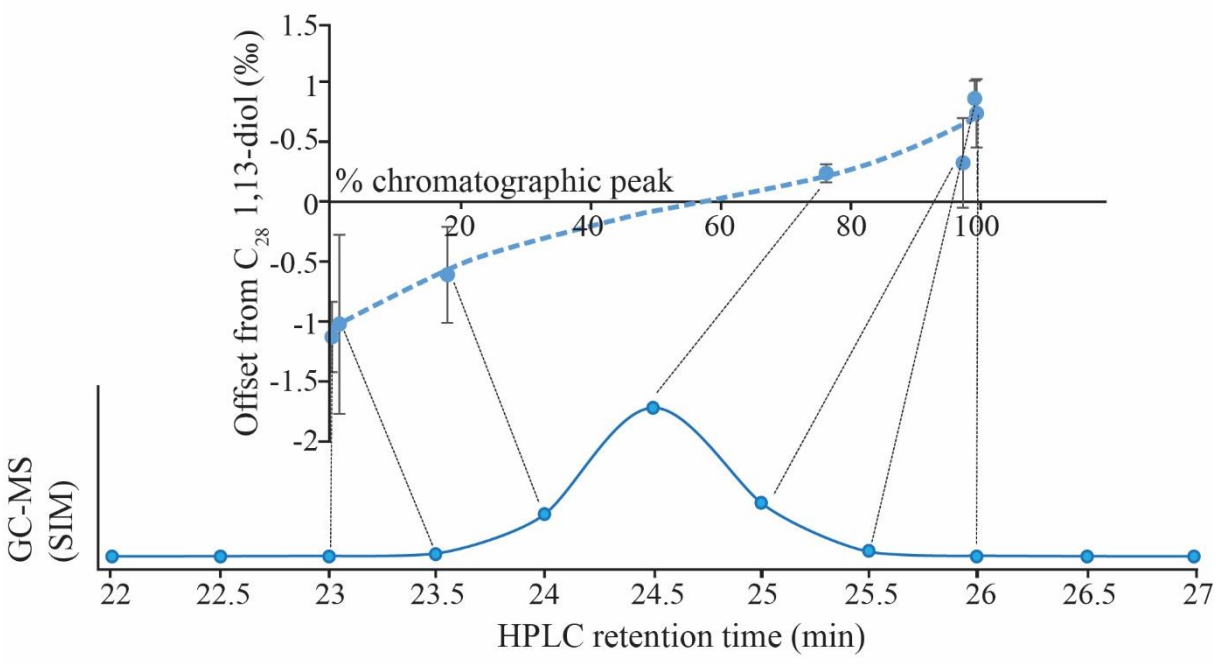
Offset from C_{28} 1,13-diol (‰)
1.5
1
-0.5
0
-0.5
-1
-1.5
-2
% chromatographic peak
20
40
60
80
100
GC-MS
(SIM)
22
22.5
23
23.5
24
24.5
25
25.5
26
26.5
27
HPLC retention time (min)

793

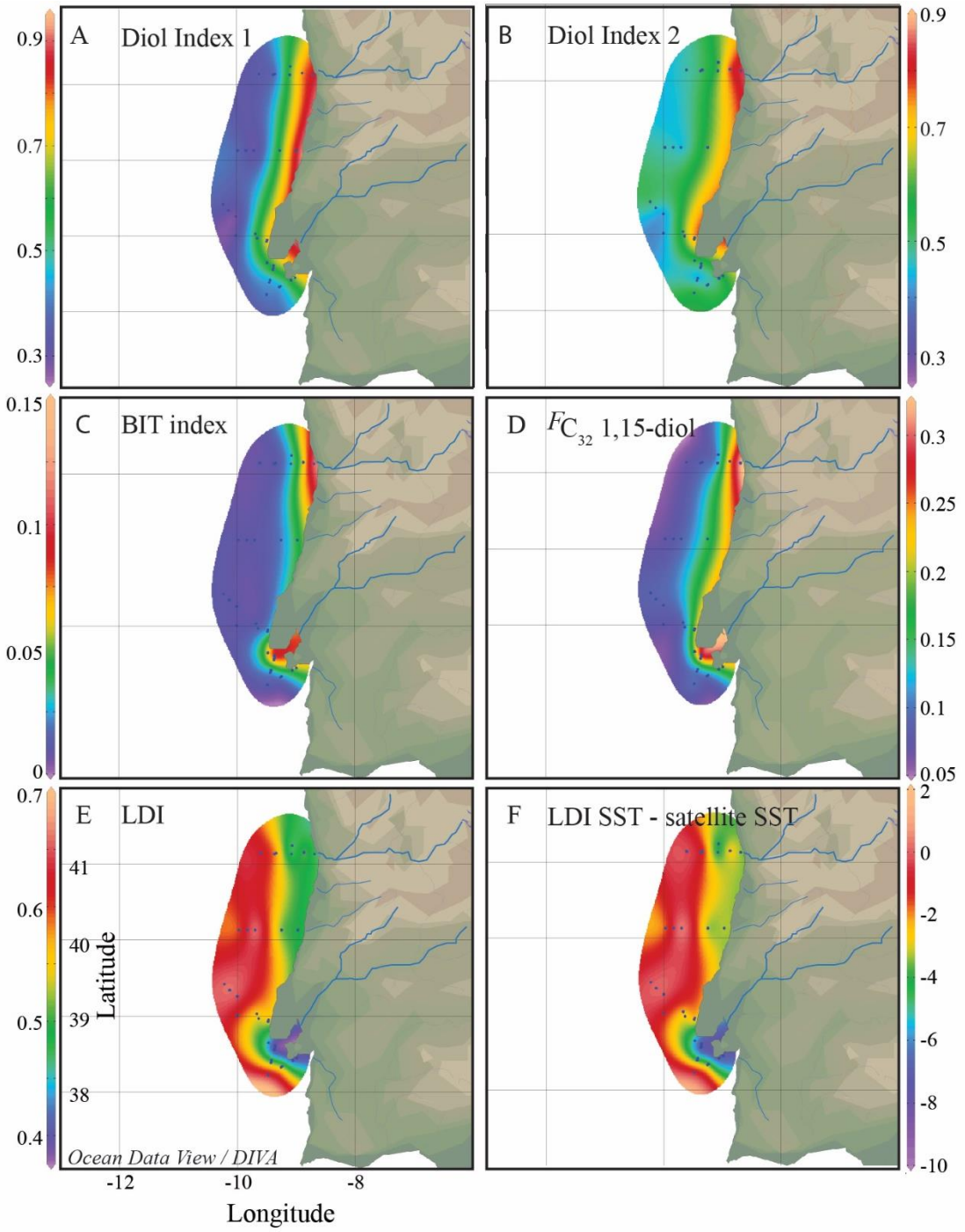
A Diol Index 1
B Diol Index 2
C BIT index
D $F_{C_{32}}$ 1,15-diol
E LDI
F LDI SST - satellite SST
Latitude
Longitude
Ocean Data View / DIVA

794

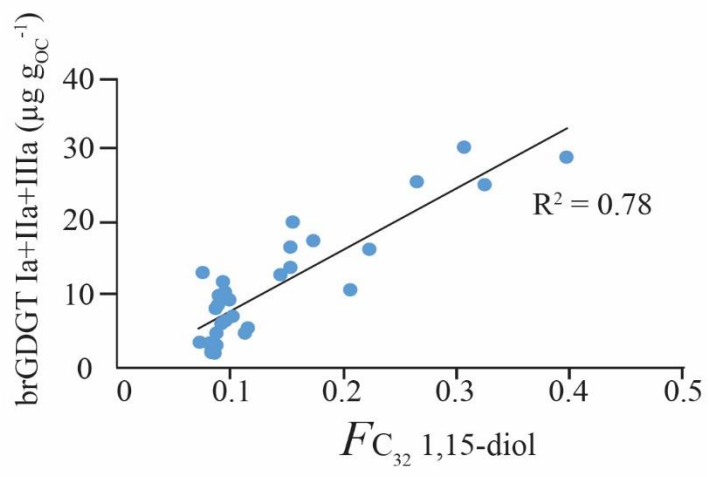
brGDGT Ia+IIa+IIIa (µg g$_{OC}^{-1}$)
40
30
20
10
0
0
0.1
0.2
0.3
0.4
0.5
R^2 = 0.78
FC$_{32}$ 1,15-diol

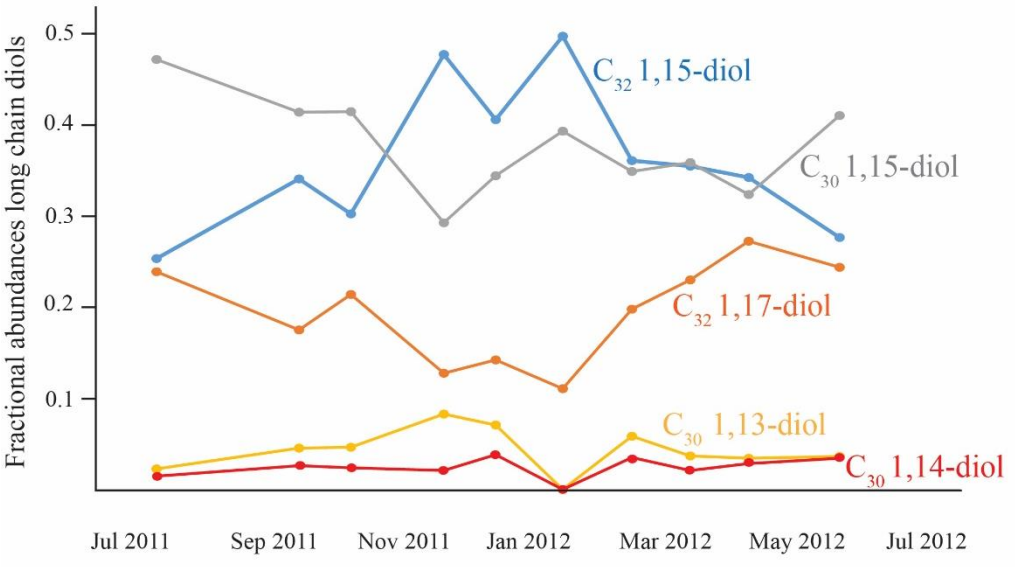
Fractional abundances long chain diols
0.5
0.4
0.3
0.2
0.1
C$_{32}$ 1,15-diol
C$_{30}$ 1,15-diol
C$_{32}$ 1,17-diol
C$_{30}$ 1,13-diol
C$_{30}$ 1,14-diol
Jul 2011
Sep 2011
Nov 2011
Jan 2012
Mar 2012
May 2012
Jul 2012

Table 1. Relative abundances of the different long chain diols and calculated indices for the different surface sediment transects. Transects are shown in Fig. 1D; the numbers indicate the sample stations, with 1 representing the station closest to the coast, and increasing further offshore. The dates for the Tagus river SPM indicate the time of sampling. n.d. = not detected.

									Indices		
	C_{28} 1,14	C_{28} 1,13	C_{30} 1,15	C_{30} 1,14	$C_{30:1}$ 1,14	C_{30} 1,13	C_{32} 1,15	C_{32} 1,17	**LDI**	**Diol Index 1**	**Diol Index 2**
Transect I											
1	n.d.	0.07	0.10	0.50	0.19	0.05	0.10	n.d.	0.46	0.84	0.82
2	n.d.	0.05	0.12	0.50	0.20	0.05	0.08	n.d.	0.55	0.80	0.83
3	n.d.	0.17	0.22	0.36	0.11	0.10	0.05	n.d.	0.45	0.62	0.58
4	n.d.	0.19	0.24	0.40	n.d.	0.12	0.06	n.d.	0.44	0.63	0.57
5	n.d.	0.15	0.48	0.25	n.d.	0.12	0.09	n.d.	0.62	0.34	0.58
6	n.d.	0.19	0.40	0.24	n.d.	0.11	0.06	n.d.	0.57	0.39	0.46
7	n.d.	0.17	0.43	0.24	n.d.	0.09	0.06	n.d.	0.63	0.36	0.48
Transect II											
1	n.d.	n.d.	0.13	0.91	n.d.	n.d.	n.d.	n.d.	-	0.87	-
2	n.d.	0.13	0.25	0.40	n.d.	0.12	0.09	n.d.	0.50	0.61	0.61
3	n.d.	0.15	0.52	0.17	n.d.	0.09	0.07	n.d.	0.69	0.25	0.42
4	0.03	0.16	0.44	0.23	n.d.	0.09	0.06	n.d.	0.63	0.36	0.49
5	n.d.	0.21	0.40	0.26	n.d.	0.08	0.05	n.d.	0.58	0.42	0.50
Transect III											
1	0.02	0.08	0.20	0.46	0.17	0.09	0.10	n.d.	0.58	0.72	0.78
2	n.d.	0.11	0.21	0.52	n.d.	0.07	0.08	n.d.	0.54	0.71	0.74
3	0.02	0.13	0.28	0.34	0.09	0.09	0.05	n.d.	0.56	0.56	0.62
4	0.03	0.18	0.28	0.33	0.03	0.09	0.06	n.d.	0.51	0.56	0.57
5	n.d.	0.17	0.45	0.20	n.d.	0.12	0.06	n.d.	0.61	0.32	0.43
6	n.d.	0.16	0.50	0.17	n.d.	0.10	0.07	n.d.	0.66	0.26	0.40
7	0.03	0.15	0.47	0.20	n.d.	0.10	0.07	n.d.	0.66	0.32	0.48
8	0.04	0.17	0.47	0.23	n.d.	0.07	0.06	n.d.	0.66	0.36	0.52
Transect IV											
1	n.d.	0.18	0.22	0.24	n.d.	0.13	0.23	n.d.	0.42	0.52	0.44
2	n.d.	0.11	0.10	0.34	0.14	0.10	0.20	n.d.	0.33	0.77	0.62
3	n.d.	0.18	0.25	0.35	n.d.	0.12	0.10	n.d.	0.45	0.60	0.56
4	n.d.	0.25	0.25	0.29	n.d.	0.12	0.10	n.d.	0.40	0.54	0.44
5	n.d.	0.24	0.33	0.23	n.d.	0.13	0.07	n.d.	0.47	0.45	0.42
6	0.03	0.18	0.35	0.25	n.d.	0.11	0.07	n.d.	0.54	0.45	0.49
7	0.04	0.13	0.40	0.26	n.d.	0.10	0.08	n.d.	0.64	0.43	0.57
Transect V											
1	0.03	0.13	0.17	0.36	0.11	0.10	0.10	n.d.	0.42	0.70	0.63
2	n.d.	0.28	0.23	0.30	n.d.	0.11	0.11	n.d.	0.38	0.56	0.44
3	0.03	0.19	0.34	0.26	n.d.	0.11	0.07	n.d.	0.53	0.46	0.49
4	0.03	0.19	0.38	0.23	n.d.	0.10	0.07	n.d.	0.57	0.41	0.48
SPM											
Tagus river											
12/07/2011	n.d.	n.d.	0.47	0.01	n.d.	0.02	0.25	0.24	-	0.03	0.39
16/09/2011	n.d.	n.d.	0.41	0.03	n.d.	0.05	0.34	0.17	-	0.06	0.36
18/10/2011	n.d.	n.d.	0.41	0.02	n.d.	0.05	0.30	0.21	-	0.05	0.34
22/11/2011	n.d.	n.d.	0.29	0.02	n.d.	0.08	0.48	0.13	-	0.07	0.20
16/12/2011	n.d.	n.d.	0.34	0.04	n.d.	0.07	0.41	0.14	-	0.10	0.35
16/01/2012	n.d.	n.d.	0.39	n.d.	n.d.	n.d.	0.50	0.11	-	-	-
17/02/2012	n.d.	n.d.	0.35	0.04	n.d.	0.06	0.36	0.20	-	0.09	0.38
16/03/2012	n.d.	n.d.	0.36	0.02	n.d.	0.04	0.35	0.23	-	0.06	0.36
12/04/2012	n.d.	n.d.	0.32	0.03	n.d.	0.03	0.34	0.27	-	0.08	0.45
24/05/2012	n.d.	n.d.	0.41	0.03	n.d.	0.04	0.28	0.24	-	0.08	0.49